

BLENDING KERNEL FUZZY LOCAL INFORMATION C-MEANS (BKFLICM) CLUSTERING BASED EDGE DETECTION FOR LUNG IMAGES

¹P. Dhanalakshmi, ²Dr. G. Satyavathy

¹Research Scholar, Department of Computer Science, Sri Ramakrishna College of Arts and science for Women, Coimbatore.

²Associate Professor, Department of Computer Science, Sri Ramakrishna College of Arts and science for Women, Coimbatore.

ABSTRACT: The medical diagnosis and clinical practice greatly demands medical image classification, an emerging area of research which includes modern medical imaging technology. Recently, Fuzzy Bat Algorithm (FBA) with Mean Weight Convolution Neural Network (MWCNN) algorithm was proposed for Region of Interest (RoI) area detection in the lung images in order to increase the classification accuracy. The image processing system outcomes are influenced by edge detection e.g. region segmentation, objects detection. Edge detection is done through Blended Kernel Based Fuzzy Local Information C-Means (BKFLICM) technique and construction of gradients in the scale is achieved by clustering of all image pixels in a feature space. The image segmentation mainly relies on the pixel intensity which is used for assessing resemblance amidst pixels. The edge detection using BKFLICM is performed by formation of new kernel range which is obtained by merging hyperbolic tangent kernel and Gaussian kernel. The special feature of BKFLICM is the fuzzy local (gray level) similarity measure through the kernel function. This does the edge detection perfectly while preserving the image details following which FBA and MWCNN classifier are utilized for segmentation and classification respectively. The training of lung image classification deprived of severe over-fitting is mainly done through MWCNN with sufficient labelled images and improved accuracy is also obtained for (LIDC-IDRI) database. The performance metrics such as accuracy, precision, recall, and F-measure values are also enhanced using the proposed algorithm which is validated by the experimental outcomes.

KEYWORDS: Lung Cancer, Multi-Scale Decomposition, Fuzzy Bat Algorithm (FBA), Mean Weight Convolution Neural Network (MWCNN), Blended Kernel Based Fuzzy Local Information C-Means (BKFLICM), clustering, edge detection, segmentation, and classification.

1. INTRODUCTION

Human lungs consist of couple of air-filled organs which is positioned on both sides of the chest. The illness caused due to the anomalous cell multiplication is referred as lung cancer and considered as world's deadliest disease [1]. A survey by the World Health Organization (WHO), reports that in 2030 [2] nearly 10 million people may be deceased due to lung cancer. The various symptoms of lung cancer are coughing, shortness of breath, wheezing and bloody mucus in case of utmost severe stage. The trachea called windpipe is the place where lung cancer originates typically and migrates towards the bronchus or lung tissue [3]. The chemotherapy, radiation and surgery are the possible treatments for curing lung cancer. CT (Computed tomography) radiography is another possible solution for recognizing the lung cancer. Following which, biopsy is involved for diagnosis which is accomplished using bronchoscopy. Mostly, men are affected and deceased because of lung cancer. Therefore developing a novel robust technique is essential for early stage diagnosis of lung cancer [4] which in turn creates vital prominence for disease diagnosis and treatment [5–6] through lung image classification. The differentiation of normal or abnormal medical images is acquired through medical image feature extraction and classification [7-9]. Medical image classification is required to narrow down the scope of search for doctors, visiting medical imaging library,

The images' elementary features such as color, texture and shape form the basis of traditional medical image classification algorithms [10,11]. The diagnosis method relies on accuracy, consistency of diagnosis, and image interpretation time. Also enormous amount of training data is required by the traditional medical classification algorithms which in turn lead to extensive processing time. The old-style diagnosis systems develop flaws such as higher error due to less volume of data. These methods are interested only in analyzing a specific organ; The CT images edge is a key factor in lung images classification. The impulsive or abrupt modification in any of the (multiple) characteristics at pixel level leads to contour medical image edges. The modification involved in

colour, texture, shade or light absorption is monitored. These characteristics might promote in assessing the orientation, size, depth and surface features in an image.

The objects boundaries contained by images are obtained using the image processing technique namely Edge detection which works on the principle of discontinuities detection in brightness. Edge detection finds its application in various fields such as image processing, computer vision, and machine vision. The Linear Time Invariant (LTI) filters are greatly utilized for the traditional edge detection techniques [12] and play a vital role in recognizing an edge as an unexpected change of grey scale pixel intensities which is well recognized and computationally proficient.

The concept of spatial differential filters utilizing local gradient is a key role in various edge detection technique such as Canny, Sobel, Robert, Kirsch, Prewitt and LOG. Though these filters are computationally efficient for data processing, they are not resistant to noise. Fuzzy Set theory does edge detection through mathematical and logical reasoning established on approximations reasonably than crisp values, thereby achieving diminished problem complexity where attainment or prediction of steady values cannot be accomplished. The edge detection is a key factor for Image segmentation which influences proper classification and increases the probability of patient's being [13].

The process of image partitioning into substantial segments which belongs to dissimilar objects is called as image segmentation and is primarily involved in medical imaging fields [14]. Global thresholding algorithm and Local/adaptive thresholding algorithms play a significant role in performing segmentation of lung images where transformation of gray scale input image to bi-level image is accomplished through various thresholding based methods [15]. The disadvantage is that variations are not taken into account for operation and not suitable for pathologic classification. Hence Fuzzy Bat Algorithm (FBA) is greatly involved in optimization of threshold value. Yet another solution is the Deep learning algorithm for mitigating the problems in medical imaging fields. Convolutional Neural Network (CNN) is one of the main deep learning techniques utilized for medical image classification [21-24]. CNN is widely used in vast applications of image pattern recognition and image classification. Blended Kernel Based Fuzzy Local Information C-Means (BKFLICM) clustering algorithm is used for lung image edge detection and then outliers of the clusters are considered as edges. It is an efficient method for edge detection and determines discontinuous edges accurately. The pixel intensity is vital for the assessment of similarity among pixels which is utilized for image segmentation. Fuzzy Bat Algorithm (FBA) with Mean Weight Convolution Neural Network (MWCNN) algorithm is suggested for Region of Interest (RoI) area detection and classification for the lung images to enhance the classification accuracy. Finally, edge detection along with classification accuracy is accomplished.

2. LITERATURE REVIEW

Noviana et al [16] suggested a technique for recognizing abnormalities in every section of entire lungs which aids in surgery planning and also establishing the nodules existence by means of axial segmentation of lungs CT scan. The various stratagem involved are image cropping, image binarization, canny edge detection and morphological operation. The separation of image area is accomplished through image cropping. A binary image consisting of two values with grey level that is black and white (ROI) is obtained via Binarization method of lungs CT scan image. The edge detection is primarily achieved through Canny Method and smoothing of lungs edge is done through Morphological operation which in turn reflects smooth edge outcome. The elimination of image background is also accomplished for obtaining the lungs main focus. Canny edge detection helps in processing the data in a comparatively diminutive time and is computationally optimized; nevertheless, they are vulnerable to noise

Qadir et al [17] utilized the concept of cellular automata for edge detection of lung CT scan images in order to diagnose the lung cancer through fully automated process. This approach is robust, more precise in lung borders detection and less costly. Li et al [18] established an enhanced detection method by creating a combination of Fuzzy Integrated Active Contour Model (FIACM)-based segmentation method and a segmentation refinement method based on Parametric Mixture Model (PMM), Cost-sensitive Support Vector Machines (C-SVM) classifier for juxta-vascular nodules for Computerized Tomography (CT) images detection of different forms of pulmonary nodules. The edge and local region information integration is mainly achieved by means of FIACM. The posterior probability forms the basis for specifying the new edge-stopping function. The model motivation power for the active contour evolution is achieved through Fuzzy energy and 2D, 3D features are utilized for C-SVM classifier. The proposed method reveals better performances which are achieved through experimental results by recognizing pulmonary nodules but precise edge detection is not accomplished.

Kaur et al [19] designed a system for edge detection which is established on fuzzy logic based algorithm through scanning it using a 2*2 pixel window and implementation is performed in MATLAB platform. The MATLAB which has Graphical User Interface (GUI) is greatly exploited in image loading and for resultant image at various transitional stages of displaying process. The outcomes are contrasted with standard edge detection algorithm such as “Canny”, “Sobel”, “Prewitt” and “Roberts”. The edge thickness is required rightly and optimization of various fuzzy parameters can be enhanced. The color image processing especially for edge detection is challenging for the suggested method.

Haq et al [20] concentrated on fuzzy logic based edge detection for both smooth and noisy clinical images which deploys 3x3 mask directed by fuzzy rule set in case of noisy images. The strengthening of smooth images is accomplished by the integration of contrast adjustment mask and edge detection mask for smooth clinical images. Sobel, Prewitt, Laplacian of Gaussian (LOG), Roberts and Canny are taken as reference and contrasted with above established edge detection techniques. The false edge pixels which are 22 in number are detected by the established edge detection technique when applied to a smooth clinical image of size 270x290 pixels having 24 dB ‘salt and pepper’ noise contrasted to Sobel (1931), Prewitt (2741), LOG (3102), Roberts (1451) and Canny (1045) false edge pixels. In the presence of smooth and noisy clinical images, the proposed method delivers upgraded solution to the edge detection problem

Kirienko et al [21] classified the lung cancer lesions as T1-T2 or T3-T4 on staging Fluorodeoxyglucose Positron Emission Tomography (FDG-PET)/CT images by evolving a CNN based algorithm. Retrospectively selected a cohort of 472 patients (divided in the training, validation, and test sets) submitted to staging FDG-PET/CT within 60 days before biopsy or surgery. There involves a bounding box on both PET and CT images in case of CNN input, gathered around the lesion centre. CNN is greatly involved in assisting the staging of patients by lung cancer. The risk stratification improvement is greatly achieved with the incorporation of patients’ clinical features in the CNN algorithm.

Zhang et al [22] suggested an approach for pulmonary nodes detection utilizing three-dimensional CNN and categorizing into malignant or benign diseases established on pathologically and laboratory proven outcomes. Remarkable sensitivity and specificity for smaller nodules (<10 mm) subgroup analysis which is same as larger nodules (10-30 mm) are also achieved. The CNN model performance is greater compared to manual assessment. It greatly supports doctors in clinical practice through additional improvement and validation in larger screening cohorts.

Teramoto et al [23] adopted a major deep learning technique namely Deep Convolutional Neural Network (DCNN) for creating an automated classification system for lung cancers in microscopic images. It comprises three convolutional layers, three pooling layers, and two fully connected layers for classification. The cropping and resampling of microscopic images is done for attaining images with resolution of 256 x 256 pixels and mitigating over-fitting. Collected images were augmented via rotation, flipping, and filtering. About 71% of the images classification is attained appropriately, which is at par with the accuracy of cytotechnologists and pathologists. In future, Ascytological diagnosis of lung cancer can be concentrated which is considered as difficult task for pathologists.

Bonavita et al [24] utilized 3D CNNs for nodule malignancy assessment and integration of automatic end-to-end existing pipeline of lung cancer detection is accomplished. Considering nodules probabilities sum of malignity in a baseline lung cancer pipeline enhanced its F1-weighted score by 14.7%, whereas integrating the malignancy model itself via transfer learning outperformed the baseline prediction by 11.8% of F1-weighted score. Though there is restriction in lung cancer datasets size, the lung cancer prediction enhancement is accomplished by incorporating predictive models of nodule malignancy.

Chandrashekar and Natraj [25] introduced a study that confers the Random Access Dual-port Memory (DRAM), based on Canny Edge Detection (CED) with proficient Save Carry Adder (CSA), Look-ahead Carry Adder (CLA) and Skip Carry Adder (CSkipA). DRAM-Optimal Adders is known to be a collective form of DRAM and effective optimal adder to enhance the performance of edge detection. This study intended for CED approach, where MATLAB reads the images of lung cell. The unified strategy of DRAM-Optimal Adder-CED comparatively enhances the overall performance of Field Programmable Gate Array (FPGA) with the rate of 22.76% in LUT, 8.47% in flip-flop, and 28.14% in slice with that of present approaches like CED-FPGA and DBRAM-CSLA-CED.

Soufi et al [26] introduced innovative edge detection algorithms exclusively for the images of mammography. For the edge detection of tumor, a fuzzy inference strategy was developed using the probabilities from Random Walk (RW). The edge operators, such as Sobel, LoG, Canny, and Roberts have been compared, through which the efficiency of the proposed strategy was depicted. Besides, the assessment was carried out on the tumor edge for additional advancement of the algorithm corresponding to the strategy of RW that reduces the edge

gradients. This study is compatible with other image processing applications as well. Santra et al [27] introduced a novel approach for edge detection called Modified Canny Edge Detection (MCED). This method has analysed diagnostic images, by which the identification of malign portions was simplified using segmentation. Ultimately, it reveals that the fuzzy based edge detection approach proves its efficiency to provide optimum results when compared to existing techniques of edge detection.

3. PROPOSED WORK

Blended Kernel-Based Fuzzy Local Information C-Means (BKFLICM) clustering is proposed for overall pixels of the image in a feature space created by the gradients in the scale. During the application of BKFLICM algorithm the new kernel range is generated to combine the two individual values of the kernel, which is utilized for edge detection. Post-process to edge detection, is the execution of segmentation and classification. The samples are gathered from the image dataset of LIDC-IDRI. The following phases are involved in the proposed framework, i.e. image decomposition into multiple scale layers, the process of segmentation based on FBA, the classification process on the basis of MWCNN. Figure 1 illustrates the comprehensive flow chart of the proposed framework.

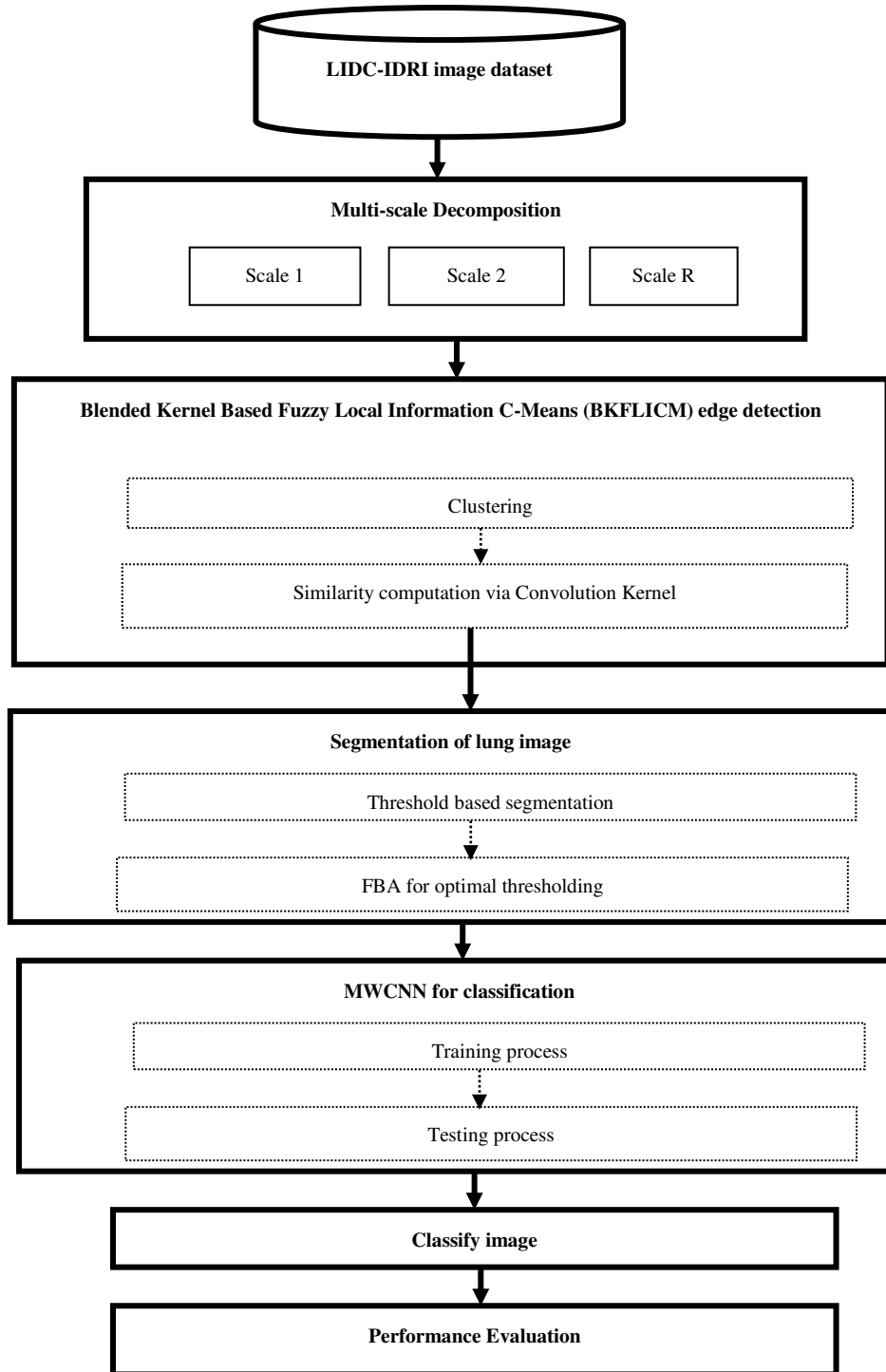


FIGURE 1. OVERALL BLOCK DIAGRAM OF THE PROPOSED SYSTEM

3.1 Decomposition of images into multiple scale layers

The process of decomposing the images into multiple scale layers on the basis of the features of spatial scale and boosting fine-scale significantly enables the derivation of image details. The conversion of multi-scale is performed by Gaussian function, besides the Gaussian filters deals with image smoothing. This process can be expressed by the following equation, in which $I(x,y)$ stands for the input image, $G(x,y,\sigma)$ indicates the Gaussian function, and $L(x, y, \sigma)$ represents the smoothed image.

$$L(x, y, \sigma) = I(x, y) * G(x, y, \sigma) \quad (1)$$

In equ(1) * specifies the convolution function. The computation of Gaussian function can be demonstrated as,

$$G(x, y, \sigma) = \frac{1}{2\pi\sigma^2} e^{-(x^2+y^2)/2\sigma^2} \quad (2)$$

Here, the variance is indicated by σ . To perform down-sampling, the images are obtained on a rough scale. The process is iterated R times, then the decomposition of diagnostic images to multi-scale layers $L = \{L_1, L_2, \dots, L_R\}$, in which image layers are denoted by R . Post-decomposition of source images, the details and noises in the images are eradicated and subdued [41]. After that, the clustering algorithm has been applied to process the edge detection.

3.2 Edge detection using Blended Kernel Based Fuzzy Local Information C-Means (BKFLICM)

Edges among the images are considered to be optical hints to accurately detect the affected regions over lung images. Clustering is presented for entire lung image pixels in a feature space created by the image gradients. To accomplish this process, the clustering algorithm, called Blended Fuzzy Local Information C-Means (BKFLICM), is used. It's an ensemble of FCM clustering using new fuzzy factor and kernel. Its objective function being integrated by the lung images' gray level information, which is expressed by,

$$J_m = \sum_{i=1}^N \sum_{k=1}^c \left[u_{ki}^m \|Im_i - v_k\|^2 + G_{ki} \right] \quad (3)$$

The estimation of fuzzy factor G_{ki} is represented by,

$$G_{ki} = \sum_{j \in N_i, i \neq j} \frac{1}{BKd_{ij} + 1} (1 - u_{kj})^m \|Im_j - v_k\|^2 \quad (4)$$

Equation 4 applies the Euclidean metric as the parameter in the objective function of FLICM, same as FCM [29]. Even though it enables the effortless computation, at times it lacks the edges in the images. This problem is overcome by presenting the kernel distance function in this study. The BKd_{jk} (Blended Kernel) is used to estimate the kernel distance. The Hyperbolic Tangent kernel is also called as Sigmoid Kernel represented as,

$$K_1(Im_j, v_k) = \tanh(v + Im_j v_k) \quad (5)$$

The subsequent equation formulates the Gaussian kernel,

$$K_2(Im_j, v_k) = \exp\left(\frac{\|Im_j - v_k\|^2}{2\sigma^2}\right) \quad (6)$$

These kernel outputs are merged by the function BKd_{jk} (Blended Kernel) and is expressed by the following equation,

$$BKd_{jk} = K_1(Im_j, v_k) \otimes K_2(Im_j, v_k) \quad (7)$$

Here, the image samples among the m -dimensional vector space is denoted by $Im = \{Im_1, \dots, Im_n\} \subseteq \mathbb{R}^m$; N is the number of images with $2 \leq c \leq N$, u_{ji} is the membership function; the weight exponent over each membership of fuzzy is represented by m ; the center of cluster's prototype is indicated by v_j ; the distance measure amidst image and cluster center is signified by BKd_{ij} . Two basic criteria for J_m objective function must be at its local minimal extreme, as regards the u_{ki} and v_k that can be attained as follows,

$$u_{ki} = \frac{1}{\sum_{j=1}^c \left(\frac{BKd_{jk} + G_{ki}}{BKd_{ij} + G_{ji}} \right)^{\frac{1}{m-1}}} \quad (8)$$

$$v_k = \frac{\sum_{i=1}^N u_{ki}^m I m_i}{\sum_{i=1}^N u_{ki}^m} \quad (9)$$

Upon convergence of the algorithm, a process of de-fuzzification is conducted, concerning the transformation of fuzzy partition matrix into a crisp partition, for which the maximum membership function is designed. During this process, the pixels are designated to the class with the maximum membership as the edge, and not an edge otherwise. This procedure is formulated as,

$$C_i = \arg_k \{\max\{u_{ki}\}\}, k = 1, \dots, c \quad (10)$$

In this way, the conversion of fuzzy image into crisp segregated image is accomplished using the proposed algorithm. As processed in the Canny edge detection approach, the Thresholding algorithm is carried out to enhance the results (e.g. make the edges thinner) of clustering. The threshold algorithm utilizes both the lower threshold values and higher threshold values during this process. Unlike the Canny approach, the threshold values rely on gradient intensity. Here, the estimation of suggested threshold values is carried out on the basis of the confidence of a pixel from the non-edge cluster. If the confidence of a pixel in the edge cluster to the non-edge cluster is lesser than the lower threshold, then it is considered as a “true” edge pixel. A pixel is considered as an edge pixel if it satisfies two criteria: its confidence to the non-edge cluster is in a range between the two thresholds and it has a spatial connection with an already established edge pixel. The rest of the pixels are concluded as non-edge pixels. The following clustering steps demonstrate the attainment of the confidence of a pixel from a cluster.

Algorithm 1. BKFLICM algorithm based edge detection for lung images

Input: A lung image I, number of clusters N.

Output: An image map that is an image with identified edges.

Step 1. Estimate the value of pixel gradient in every image channel.

Step 2. Establishing a pixel as a point that is made up of the values of gradient in lung images’ feature space.

Step 3. Classify the points into N clusters using BKFLICM algorithm

3.1. Define the number of the cluster prototypes, fuzzification parameter m and the stopping condition ϵ .

3.2. Activate the fuzzy partition matrix arbitrarily.

3.3. Define the loop counter $b=0$.

3.4. Determine the cluster prototypes through equation (9).

3.5. Estimate membership values through equation (8).

3.6. Calculate the new kernel distance through equation (7)

3.7. Stop, if $\max\{U^{(b)} - U^{(b+1)}\} < \epsilon$. Else, set $b=b+1$ and operate step 3 and 4.

Step 4. Refine the clustering results using canny edge detection.

Step 5. Choose the cluster with highest population as non-edge cluster and unite the remaining clusters as an edge cluster.

Step 6. Map the thresholding algorithm to refine the outputs from Step 5.

3.3. Segmentation Using FBA

The process of segmentation implemented through the Fuzzy Bat Algorithm (FBA) is to identify the area of the Region of Interest (RoI) among lung images. The segmentation of RoI is the initial process with the lung CT image, which enables the analysis to diagnose a cancer, tumour or other pathological conditions. All the detection approaches of lung abnormalities can be enhanced by the proficient lung segmentation strategy, concerning their accuracy and the decision value of confidence [30]. On the other hand, the primary process of image thresholding includes the optimal thresholding. Post-edge detection process, the CT image consists of two

significant pixel groups, i.e. i) high-intensity pixels found in the body, ii) low-intensity pixels positioned in the lung. This process is performed in the following way: Consider the threshold value as Th_i at step i , and let the average intensity value of body pixels be t_b , t_n , and set t_b with higher intensity than Th_i , and t_n with lower intensity than Th_i . Here, $Th_{i+1}=(t_b+t_n)/2$ is the threshold for step $i+1$. This function is iterated upto convergence. The median gray level is represented by setting the initial threshold Th_0 to 120. After convergence, the threshold value of the image is denoted by Th_k . Each pixel that possesses a higher intensity than Th_k is set to 0 which are pixels owned by body, and remaining pixels are set to 1 that exists in surrounding air. At this point, FBA effectively process the segmentation of RoI area by automatically choosing the threshold Th_i . Besides, Bat algorithm functions on the basis of bat's echolocation characteristic [31] [41]. The bats emit the louder noise pulse and hear the echo returns from the intensive objects, by which the bats are enabled to hunt their food, besides they avoid their on-way hurdles, which are collectively termed as echolocation. Based on this, the RoI is accurately segmented by estimating the fitness values[41]. Throughout this study, the performance of the algorithm is enhanced by executing the fuzzy method, as it regulates the parameters of BA effectively.

3.4. Mean Weight Convolution Neural Network (MWCNN) Algorithm For Classification

The lung image dataset (LIDC-IDRI) is used for the proposed Mean Weight Convolution Neural Network (MWCNN) classifier, through which it is observed that a neural network is nourished with number of features, from which the machine could learn many information to obtain the optimal result [32]. The following layers are included in the proposed classifier:

Input layers: As a training image, the segmented lung image is received by Input layer. Then the Input layer converts the data as a combined one, in terms of processing it to the subsequent layer in an appropriate way.

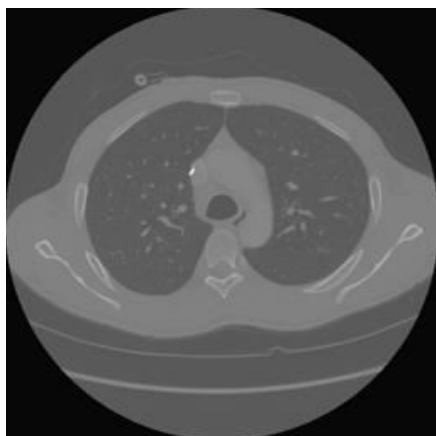
Convolutional Layers: These layers act as feature extractors, as they observe the feature representations of the segmented lung images provided as input. In a feature map, every neuron contains an accessible area that has correlated to a neuron's neighbourhood in the preceding layer using a set of trainable mean weights, also called as a filter bank [33].

Pooling Layers: Pooling layers is used for the reduction of spatial resolution in the feature maps which helps in obtaining the spatial invariance's into input distortions and translations [34]. During this research, the pooling function in the process of classification has delivered each sub-sampled region's average rounded value of the integer.

Fully Connected Layers: A number of convolutional layers and pooling layers are piled on top of each other for the withdrawal of additional abstract feature representations while processing through the network. These layers are followed by the fully connected layers for deducing those feature representations and processing the task of high-level reasoning [35]. On top of the layer, the softmax operator has been applied by the proposed classifier [36]. As a classifier, the Radial Basis Functions (RBFs) is used on top of the convolutional layer that considerably augments the accuracy of classification[41].

4. EXPERIMENTAL RESULTS

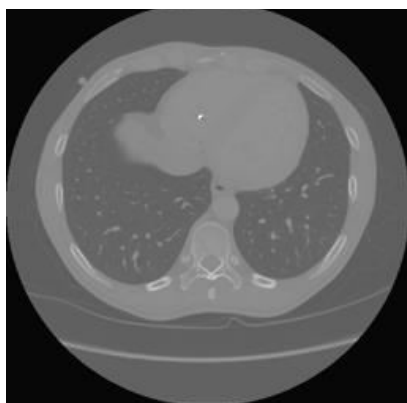
During this study, the Lung Image Database Consortium (LIDC-IDRI) dataset is considered for the classification of lung images, which is a multitude of diagnostic and lung cancer screening thoracic Computed Tomography (CT) scans that accompanies marked-up annotated lesions. This is an online-based global platform that exclusively eases the process of lung cancer detection and diagnosis, concerning the improvement, practice, and assessment on the approaches of Computer-Assisted Diagnostics (CAD). The implementation process includes 200 images that are derived from LIDC-IDRI, out of which 150 images are trained, and 50 have been tested. The images are gathered from URL: <https://wiki.cancerimagingarchive.net/display/Public/LIDC-IDRI> [37], the LIDC-IDRI-0068 belongs to class 3 - malignant metastatic, the LIDC-IDRI-0149 belongs to class 1- benign or non-malignant disease, and the LIDC-IDRI-0173 belongs to class 0 - No disease. The details of images that are used for implementation are shown in table 1. Figure 2(a-f) shows the input image samples and edge detection results of three classes.



(a) Input image belongs to 0=No disease (0173)



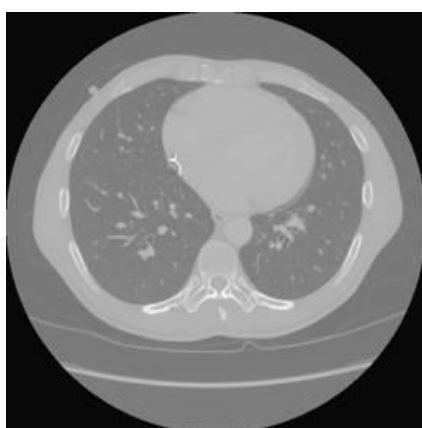
(b) Edge detection results belongs to 0=No disease (0173)



(c) Input image belongs to 1=benign or non-malignant disease(149)



(d) Edge detection results belongs to 1=benign or non-malignant disease(149)



(e) Input image belongs to 3 = malignant metastatic (168)



(f) Edge detection results belongs to 3 = malignant metastatic (168)

FIGURE 2. EDGE DETECTION IMAGE RESULTS

TABLE 1. SAMPLES USED FOR LUNG IMAGES CLASSIFICATION

FILE NAME	NUMBER OF IMAGES	CLASS
LIDC-IDRI-0173	50	0
LIDC-IDRI-0149	70	1
LIDC-IDRI-0068	80	3

The implementation is done for various algorithms with and without edge detection. The performance parameters evaluated are Precision, Recall, Accuracy, and F-Measure for Artificial Neural Network (ANN), Support Vector Machine (SVM), Enhanced Particle Swarm Optimization Kernel Support Vector Machine (EPSOKSVM), and Fuzzy Bat Algorithm with MWCNN (FBA with MWCNN).

4.1. EDGE DETECTION METRICS

The Edge Detection approaches, specifically the Canny Edge Detection (CED), Laplacian of Gaussian (LoG), Fuzzy Logic Based Edge Detection (FLED) and the proposed BKFLICM algorithm are compared, based on the metrics, such as Mean Squared Error (MSE), Peak Signal-To-Noise Ratio (PSNR) and Structural Similarity Index (SSIM). Nevertheless, the evaluation reveals that these methods solely orient on entire image quality, and are incompetent to understand the quality of edges.

A weighted function of deviations in images/square difference among compared images is called MSE [38]. Equation (11) represents the image size as M and N, and indicates the locations as $I_1(i,j)$ and $I_2(i,j)$.

$$MSE = \frac{1}{MN} \sum_{i=1}^M \sum_{j=1}^N (I_1(i,j) - I_2(i,j))^2 \quad (11)$$

The PSNR metric that has the sturdy association with MSE, is expressed in Equation (12), by which the level of losses/integrity of signals is represented [39].

$$PSNR = 10 \log \left(\frac{\max(I)^2}{MSE} \right) \quad (12)$$

Despite the extensive use of these measures, the images with varied distortion levels may possess the identical values of PSNR and MSE [39]. SSIM has close association with the visual system of human, since it separates the valuable details like luminance (l), contrast(c) and structure (s), by which the evaluation of structure preservation and noise removal are enabled [40].

$$SSIM = function (l(I_1, I_2), c(I_1, I_2), s(I_1, I_2)) \quad (13)$$

The usage of commonly used metrics, such as MSE, PSNR and SSIM is inadequate to prove the edge performance in images. The comparison of implementation results obtained for several metrics for the edge detection approaches are presented in Table 2.

TABLE 2. EDGE DETECTION METHODS RESULTS COMPARISON vs. METRICS

METRICS	EDGE DETECTION METHODS			
	CED	LOG	FLED	BKFLICM
MSE	12.76	10.13	8.25	5.44
PSNR (dB)	37.69	41.58	46.85	54.89
SSIM	0.7528	0.7962	0.8528	0.9218

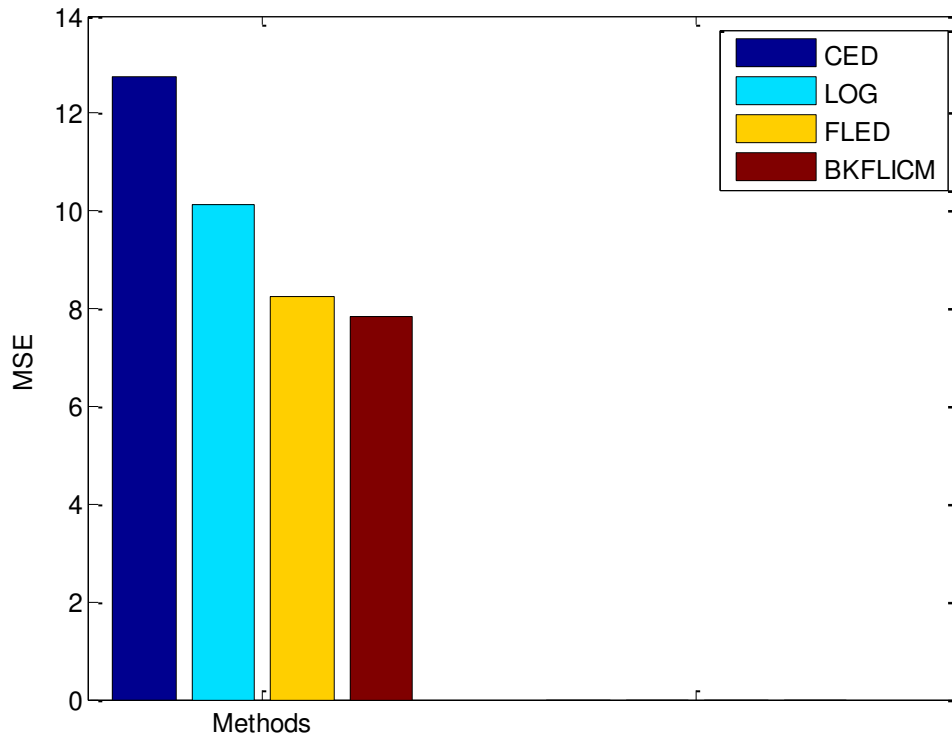


FIGURE 3.MSE RESULTS COMPARISON VS. EDGE DETECTION METHODS

Figure 3 compares the MSE outcomes of the edge detection methods, specifically CED, LOG, FLED and BKFLICM. The comparison graph depicts that the proposed BKFLICM has a minimum MSE ratio of 7.84. On the other hand, the higher MSE ratio of 12.76, 10.13, and 8.25 are obtained for the existing approaches CED, LOG and FLED respectively which is represented in Table 2. Compared to other strategies, the proposed approach accomplishes the proper identification of edges through FLICM using kernel distance method.

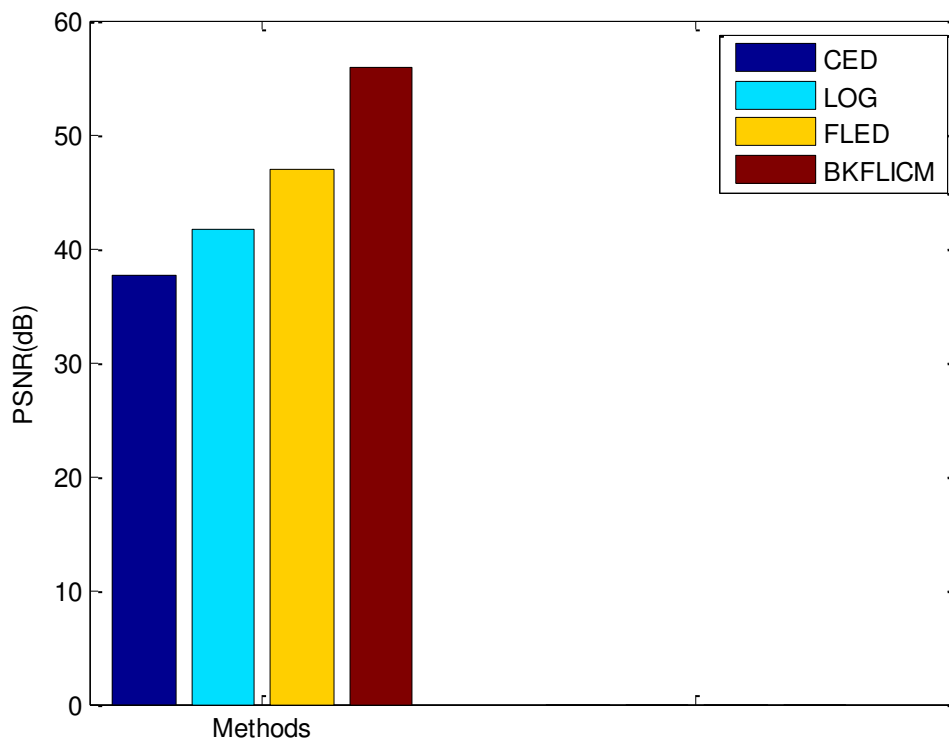


FIGURE 4.PSNR RESULTS COMPARISON VS. EDGE DETECTION METHODS

In Figure 4, the graph compares the PSNR outputs of the edge detection methods. The proposed BKFLICM algorithm achieves greater PSNR ratio of 55.91 dB while, the existing approaches of CED, LOG and FLED have reduced PSNR ratio of 37.69 dB, 41.58 dB and 46.85 dB respectively as demonstrated in Table 2.

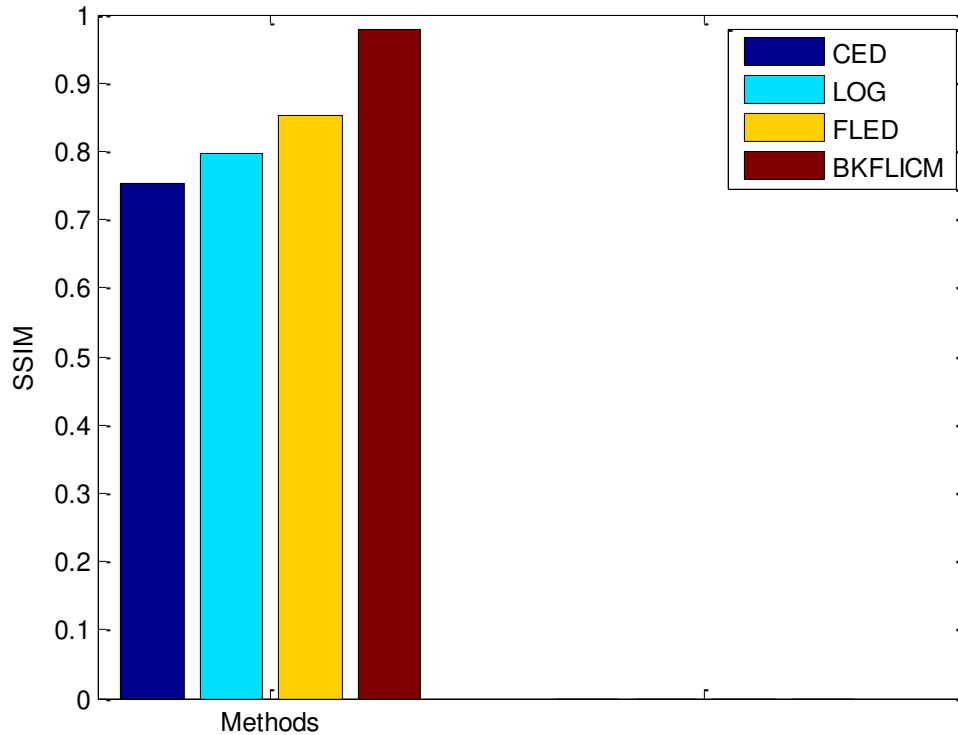


FIGURE 5. SSIM RESULTS COMPARISON VS. EDGE DETECTION METHODS

Figure 5 compares the SSIM outputs of the edge detection methods, in which the proposed BKFLICM algorithm secures superior PSNR0.9778, while the lower PSNR of 0.7528, 0.7962, and 0.8528 are attained by the existing approaches CED, LOG and FLED correspondingly as demonstrated in Table 2.

4.2. CLASSIFICATION METRICS

Precision, Recall, Accuracy, and F-Measure are the assessed metrics. Comparison of these metrics in pre and post edge detection stages of classification algorithm is done. This helps to determine the influence of the classification techniques with the edge detection algorithm.

Precision is considered as the probability of positive prediction done by the classifier is positive. Comprehensively, the high precision signifies the extremely appropriate results yielded by the algorithm instead of inappropriate. During the classification of a class, the precision is represented by the number of true positives divided by the overall quantity of elements labelled as appropriate to the positive class. The precision can be expressed as follows,

$$Precision = \frac{T_p}{T_p + F_p} \quad (14)$$

Recall is the fraction of the total amount of relevant images that were actually predicted as correct. The computation of recall can be expressed as,

$$Recall = \frac{T_p}{T_p + F_n} \quad (15)$$

As a single metric, the F-Measure unites the precision and recall through their harmonic mean. The F-Measure lies between 0 and 1, where 1 indicates the ideal and 0 signifies the worst. The harmonic mean is completely contrasted from arithmetic mean which is always intended for the least among the two elements. The following equation expresses F-Measure,

$$F - \text{measure} = \frac{2 * \text{Precision} * \text{Recall}}{\text{Precision} + \text{Recall}} \quad (16)$$

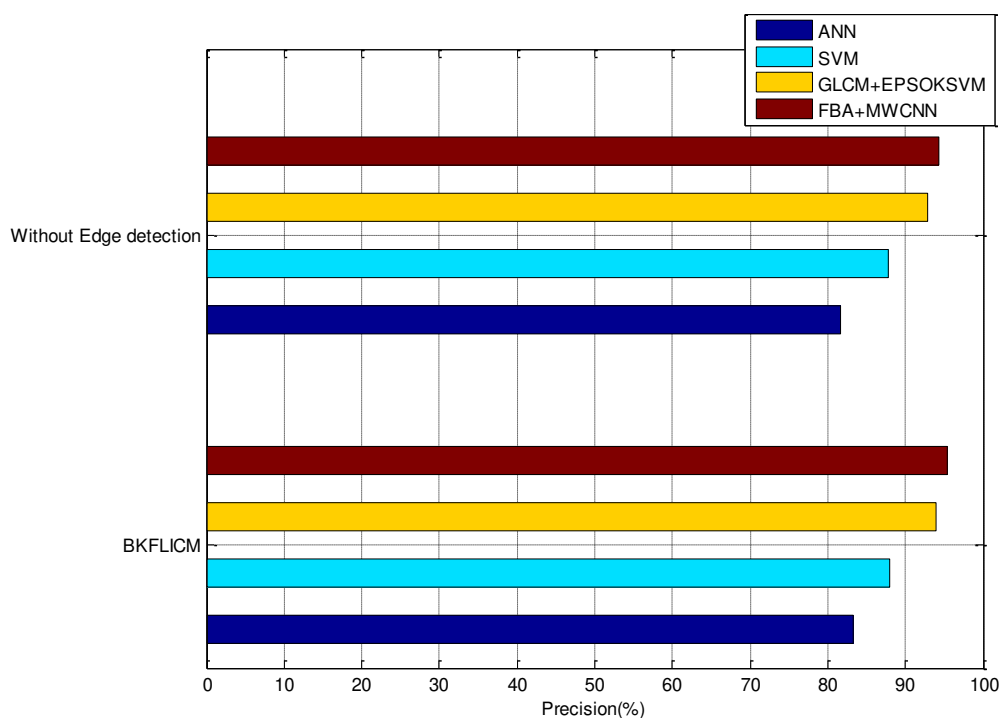
Accuracy is a parameter that helps to assess the classification approaches. The computation of accuracy is expressed by,

$$\text{Accuracy} = \frac{T_p + T_n}{(T_p + T_n + F_p + F_n)} \quad (17)$$

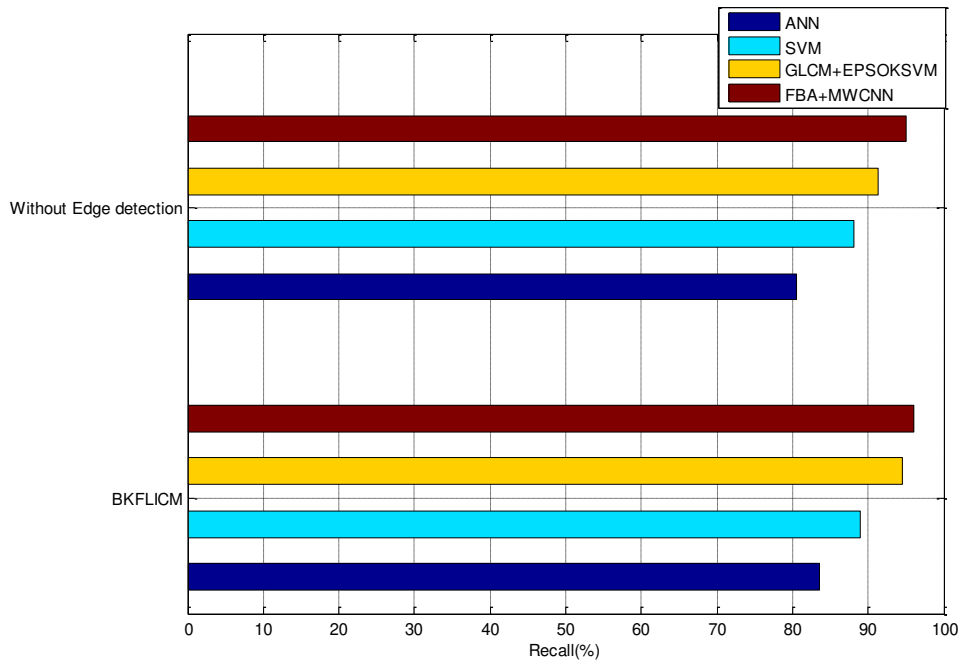
Table 3 demonstrates the comparison of performance metrics for various classifiers with and without edge detection.

TABLE 3. RESULT COMPARISON OF DIFFERENT CLASSIFIERS WITH AND WITHOUT BKFLICM EDGE DETECTION

METRICS (%)	Without Edge detection				BKFLICM based Edge detection			
	ANN	SVM	EPSOKSVM	MWCNN	ANN	SVM	EPSOKSVM	MWCNN
PRECISION	81.64	87.76	92.83	94.32	83.319	88	93.99	95.39
RECALL	80.55	88.05	91.38	95.00	83.525	89	94.46	96.014
F-MEASURE	81.09	87.91	91.71	95.00	83.42	88.126	94.22	95.702
ACCURACY	80.00	88.18	91.82	94.55	84.08	89	94.52	96.02
ERROR	20.00	11.82	8.18	5.45	15.92	11	5.47	3.98



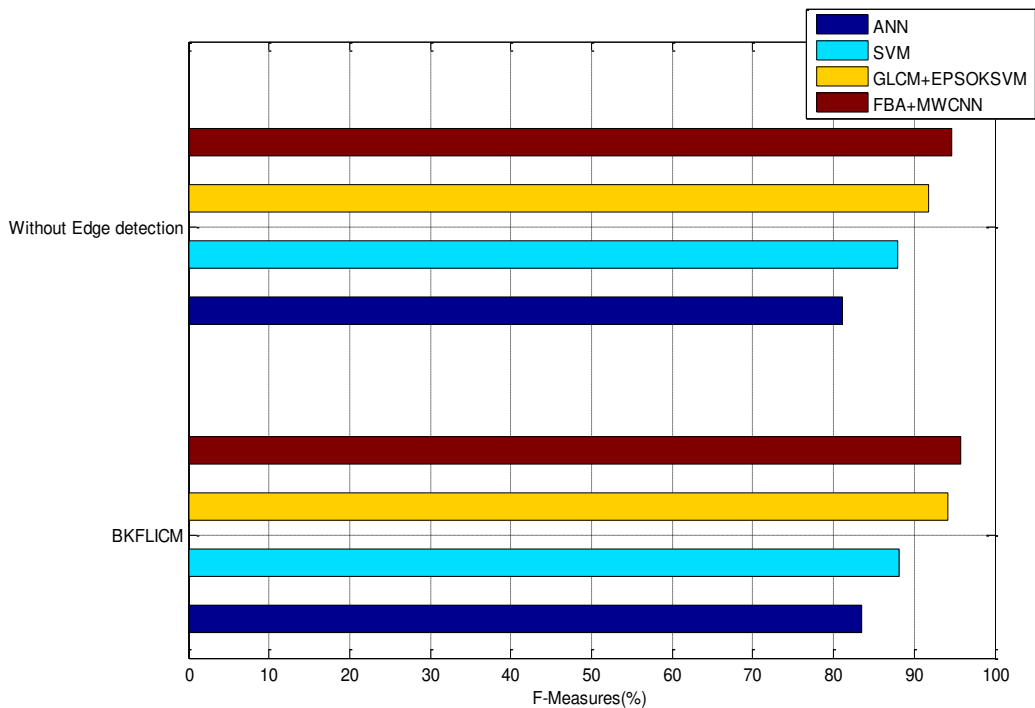
(a) PRECISION RESULTS COMPARISON



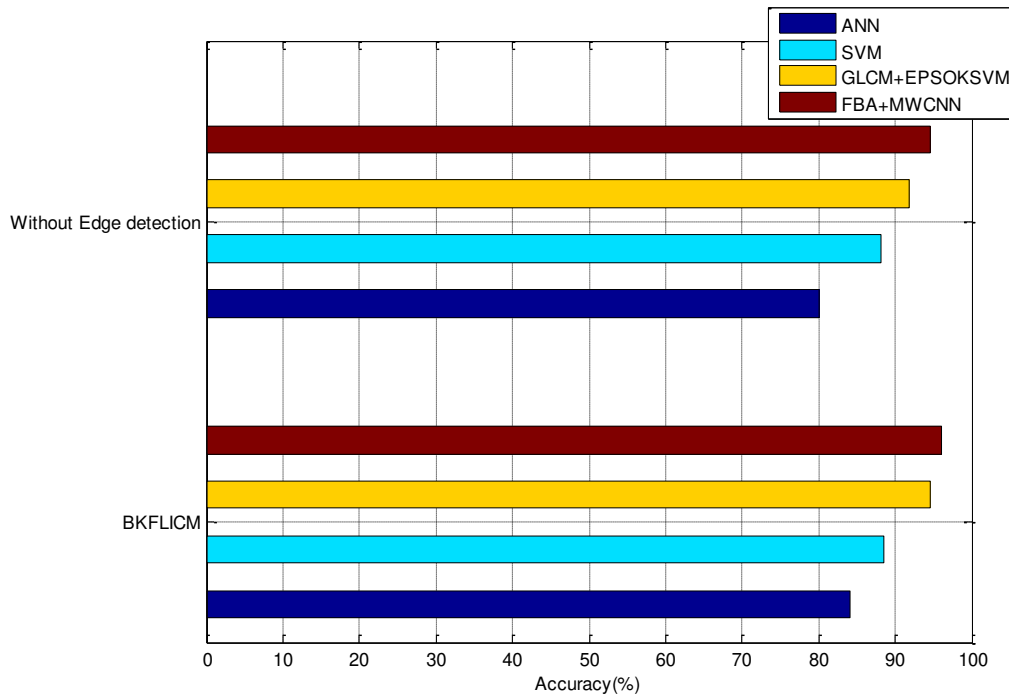
(b) RECALL RESULTS COMPARISON

FIGURE 6.PRECISION AND RECALL COMPARISON FOR DIFFERENT CLASSIFIERS WITH AND WITHOUT EDGE DETECTION

Figure 6 (a), and (b) individually compares the ratio of Precision, and Recall for the classifiers ANN, SVM, EPSOKSVM and MWCNN with and without edge detection. The results depict that the suggested classifier called MWCNN is capable of delivering the remarkable Precision rate of 95.39%, and Recall rate of 96.014% with proposed edge detection algorithm when compared to existing classifiers, as specified in Table 3. The proposed system has 12.071%, 7.39%, and 1.4% higher precision results and 12.489%, 7.014%, and 1.554% higher recall results when compared to ANN, SVM, EPSOKSVM methods respectively.



(a) F-MEASURE RESULTS COMPARISON



(b) ACCURACY RESULTS COMPARISON

FIGURE 7. F-MEASURE AND ACCURACY COMPARISON FOR DIFFERENT CLASSIFIERS WITH AND WITHOUT EDGE DETECTION

In Figure 7 (a), and (b) the rate of F-Measure and accuracy are individually compared for the classifiers ANN, SVM, EPSOKSVM, and MWCNN with and without edge detection. The results depict that the suggested MWCNN classifier provides the notable F-Measure rate of 95.70%, and accuracy rate of 96.02% with proposed edge detection algorithm than existing classifiers, as indicated in Table 3. The proposed system has 12.28%, 7.58%, and 1.48% higher F-Measure results and 11.94%, 7.02%, 1.5% higher accuracy results when compared to ANN, SVM, EPSOKSVM methods respectively.

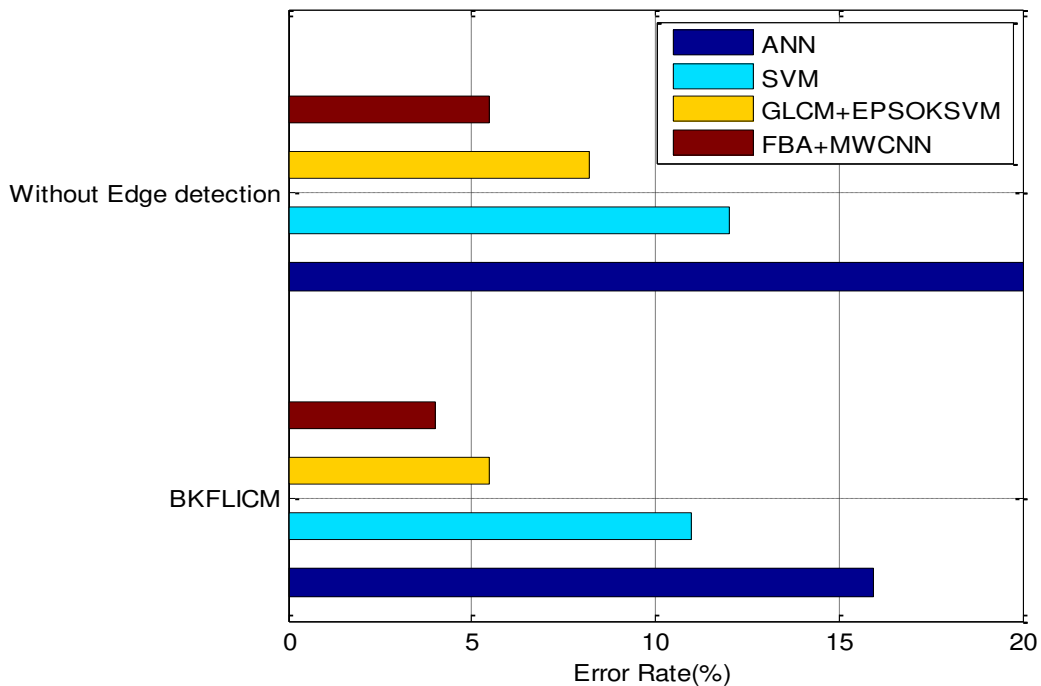


FIGURE 8. ERROR RATE RESULTS COMPARISON FOR DIFFERENT CLASSIFIERS WITH AND WITHOUT EDGE DETECTION

Figure 8 demonstrates the comparison graph of Error metric for the classifiers, namely ANN, SVM, EPSOKSVM, and MWCNN that accompanies BKFLICM edge detector and devoid of the edge detection. The outcomes signify that the suggested classifier of MWCNN procures comparatively least error ratio of 3.37% with LIDC-IDRI dataset than existing classifiers, as represented in Table 3.

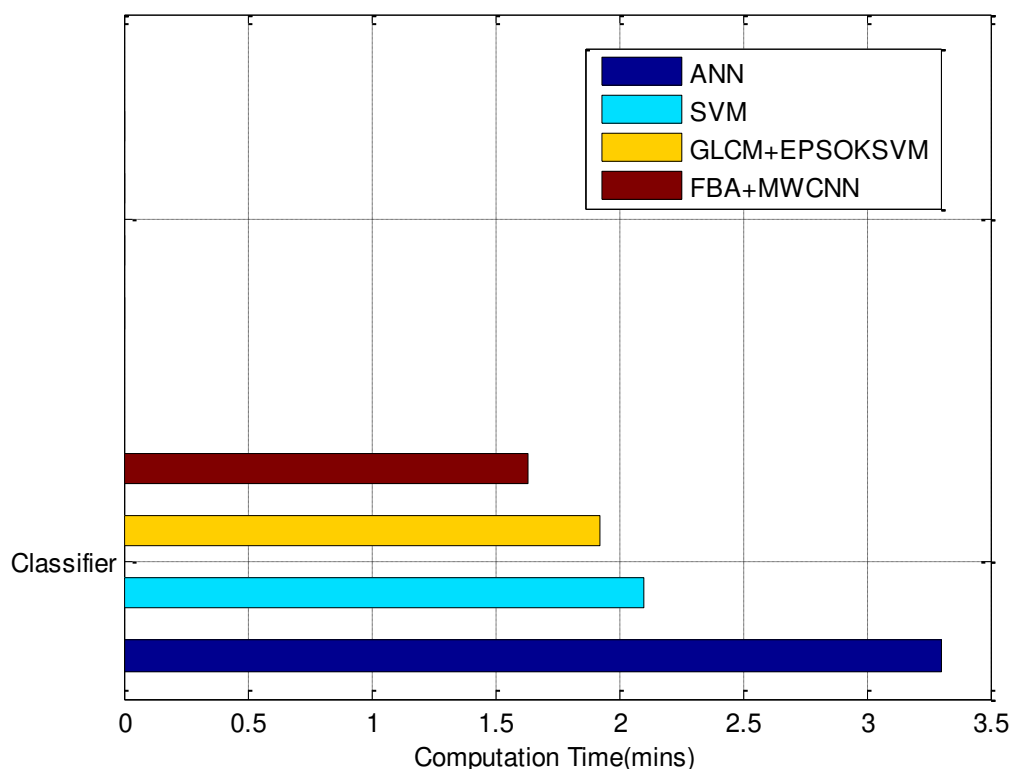


FIGURE 9. COMPUTATION TIME COMPARISON FOR DIFFERENT CLASSIFIERS

Figure 9 demonstrates the comparison graph of computation time for the classifiers ANN, SVM, EPSOKSVM, and MWCNN. These classifiers have been measured without edge detection. The outcomes signify that the proposed MWCNN classifier consumes least computation time of 1.63 mins when compared to existing classifiers for LIDC-IDRI dataset. The methods like ANN, SVM, and EPSOKSVM takes only 3.30 mins, 2.10 mins, and 1.92 mins correspondingly.

5. CONCLUSION AND FUTURE WORK

Edge detection is particular among the significant approaches for classification of Lung Image. During this research, the outputs of edge detection are improved by the novel clustering algorithm, called Blended Fuzzy Local Information C-Means (BKFLICM), derived by enhancing the FLICM clustering using new fuzzy factor and kernel. This BKFLICM algorithm is proposed for entire lung image pixels in a feature space created by the image gradients and extracted over the appropriate approximation of the variation in edge and non-edges. Hence, this algorithm is able to deliver an optimum representation of edges than the conventional Edge Detection approaches, as they provide the values based on intensity. The outcomes reveal the reduction of noise effects while retaining the great details in edges of the lung images. The comparisons between the proposed BKFLICM clustering-based edge detection algorithms and the conventional approaches are made, by considering the parameters, such as Mean Squared Error (MSE), Peak Signal-To-Noise Ratio (PSNR), and Structural Similarity Index (SSIM). The empirical findings of the comparison depicts that the proposed approach of BKFLICM proved its efficiency in Edge Detection of the lung images than all other strategies. The BKFLICM approach delivers a higher ratio of Accuracy, Precision, Recall, and F-Measure with all the classifiers of ANN, SVM, EPSOKSVM, and MWCNN. Nevertheless, the utilization of the present study includes the possibility of a reduction in the image quality, due to its inadequacy to identify the noises appropriately. In an upcoming study, this issue can be resolved by focusing on denoising strategies to eradicate the noise. Furthermore, the results of Edge Detection can be improved through determining the number of clusters N . Future work can focus to introduce a method to reconstruct the entire boundaries of lung to define the candidate cancer area.

REFERENCES

1. Siegel R, Naishadham D, Jemal A (2013). Cancer statistics. *CA Cancer J Clin*, 63, 11-30.
2. World Health Organization (2011). Description of the global burden of NCDs, their risk factors and determinants, Burden: mortality, morbidity and risk factors, Geneva, Switzerland: World Health Organization, 2011, pp 9-32.
3. Wu D, Lu L, Bi J, et al (2010). Stratified learning of local anatomical context for lung nodules in CT images. *IEEE Trans Med Imaging*, 25, 2791–98.
4. B. Rani, A. K. Goel, and R. Kaur, “A modified approach for lung cancer detection using bacterial forging optimization algorithm,” *International Journal of Scientific Research Engineering and Technology*, vol. 5, no. 1, 2016.
5. Wei L, Tang J, Zou Q. Local-DPP: an improved DNA-binding protein prediction method by exploring local evolutionary information[J]. *Inf Sci*2017;384:135–44.
6. Su R, Zhang C, Pham TD, Davey R, Bischof L, Vallotton P, Sun C. Detection of tubule boundaries based on circular shortest path and polar-transformation of arbitrary shapes[J]. *J Microsc* 2016;264(2):127–42.
7. Wei L, Zou Q. Recent progress in machine learning-based methods for protein fold recognition[J]. *Int J Mol Sci* 2016;17(12):2118.
8. Liu B, Wu H, Zhang D, Wang X, Chou K. Pse-analysis: a python package for DNA/RNA and protein/peptide sequence analysis based on pseudocomponents and kernel methods[J]. *Oncotarget* 2017.
9. Hafner M, Liedlgruber M, Uhl A. Color treatment in endoscopic image classification using multi-scale local color vector patterns[J]. *Med Image Anal*2012;16:75–86.
10. Lashari SA, Ibrahim R. A framework for medical images classification using soft set[J]. *Procedia Technol* 2013;11:548–56.
11. Yang, J. and Zhu, S.J., 2012, Narrowing semantic gap in content-based image retrieval. In 2012 International Conference on Computer Distributed Control and Intelligent Environmental Monitoring, pp. 433-438.
12. Amer, G.M.H. and Abushaala, A.M., 2015, March. Edge detection methods. In 2015 2nd World Symposium on Web Applications and Networking (WSWAN) ,pp. 1-7.
13. Zaitoun, N.M. and Aqel, M.J., 2015. Survey on image segmentation techniques. *Procedia Computer Science*, 65, pp.797-806.
14. Masood, S., Sharif, M., Masood, A., Yasmin, M. and Raza, M., 2015. A survey on medical image segmentation. *Current Medical Imaging*, 11(1), pp.3-14.
15. Sharma, N. and Aggarwal, L.M., 2010. Automated medical image segmentation techniques. *Journal of medical physics/Association of Medical Physicists of India*, 35(1), pp.3-14.
16. Noviana, R., Febriani, Rasal, I. and Lubis, E.U.C., 2017, Axial segmentation of lungs CT scan images using canny method and morphological operation. In AIP Conference Proceedings (Vol. 1867, No. 1, p. 020022). AIP Publishing LLC.
17. Qadir, F., Peer, M. and Khan, K., 2012. Efficient edge detection methods for diagnosis of lung cancer based on two-dimensional cellular automata. *Advances in Applied Science Research*, 3(4), pp.2050-2058.
18. Li, B., Chen, K., Tian, L., Yeboah, Y. and Ou, S., 2013. Detection of pulmonary nodules in CT images based on fuzzy integrated active contour model and hybrid parametric mixture model. *Computational and mathematical methods in medicine*, Vol.2013 ,no. 515386 , pp.1-15.
19. Kaur EK, Mutenja V, Gill EIS. Fuzzy logic based image edge detection algorithm in MATLAB. *International Journal of Computer Applications*. 2010; 1(22):55–58.
20. Haq, I., Anwar, S., Shah, K., Khan, M.T. and Shah, S.A., 2015. Fuzzy logic based edge detection in smooth and noisy clinical images. *PloS one*, 10(9), p.e0138712.
21. Kirienko, M., Sollini, M., Silvestri, G., Moggetti, S., Voulaz, E., Antunovic, L., Rossi, A., Antiga, L. and Chiti, A., 2018. Convolutional neural networks promising in lung cancer T-parameter assessment on baseline FDG-PET/CT. *Contrast Media & Molecular Imaging*, 2018, vol. 2018 ,no.1382309, pp.1- 6 .
22. Zhang, C., Sun, X., Dang, K., Li, K., Guo, X.W., Chang, J., Yu, Z.Q., Huang, F.Y., Wu, Y.S., Liang, Z. and Liu, Z.Y., 2019. Toward an expert level of lung cancer detection and classification using a deep convolutional neural network. *The Oncologist*, 24(9), pp.1159-1165.
23. Teramoto, A., Tsukamoto, T., Kiriya, Y. and Fujita, H., 2017. Automated classification of lung cancer types from cytological images using deep convolutional neural networks. *BioMed research international*, 2017, Vol. 2017, no. 4067832, pp.1- 6 .
24. Bonavita, I., Rafael-Palou, X., Ceresa, M., Piella, G., Ribas, V. and Ballester, M.A.G., 2020. Integration of convolutional neural networks for pulmonary nodule malignancy assessment in a lung cancer classification pipeline. *Computer methods and programs in biomedicine*, 185, p.105172.

25. Chandrashekar, N.S. and Natraj, K.R., 2018, Detection of Lung Cancer by Canny Edge Detector for Performance in Area, Latency. In 2018 International Conference on Electrical, Electronics, Communication, Computer, and Optimization Techniques (ICEECCOT) ,pp. 690-696.
26. Soufi, M., Kamali-Asl, A., Geramifar, P., Abdoli, M. and Rahmim, A., 2016. Combined fuzzy logic and random walker algorithm for PET image tumor delineation. Nuclear medicine communications, 37(2), pp.171-181.
27. Santra, S., Mandal, S., Das, K., Bhattacharjee, J. and Roy, A., 2019, A Modified Canny Edge Detection Approach to Early Detection of Cancer Cell. In 2019 3rd International Conference on Electronics, Materials Engineering & Nano-Technology (IEMENTech) ,pp. 1-5.
28. Zhang, R., Shen, J., Wei, F., Li, X. and Sangaiah, A.K., 2017. Medical image classification based on multi-scale non-negative sparse coding. Artificial intelligence in medicine, 83, pp.44-51.
29. SteliosKrinidis and VassiliosChatzis, "A Robust Fuzzy Local Information C-Means Clustering Algorithm", IEEE transactions on image processing, vol. 19, no. 5, 2010, pp. 1328-1338.
30. Xiao, X., Zhao, J., Qiang, Y., Wang, H., Xiao, Y., Zhang, X. and Zhang, Y., 2018. An automated segmentation method for lung parenchyma image sequences based on fractal geometry and convex hull algorithm. Applied Sciences, vol.8, no.5, pp.1-16.
31. Pérez, J., Valdez, F. and Castillo, O., 2015. A new bat algorithm with fuzzy logic for dynamical parameter adaptation and its applicability to fuzzy control design. In Fuzzy Logic Augmentation of Nature-Inspired Optimization Metaheuristics , pp. 65-79.
32. Ghamisi, P., Chen, Y. and Zhu, X.X., 2016. A self-improving convolution neural network for the classification of hyperspectral data. IEEE Geoscience and Remote Sensing Letters, vol.13, no.10, pp.1537-1541.
33. LeCun, Y., Bengio, Y., & Hinton, G. (2015). Deep learning. Nature, vol.521, no.7553, pp.436– 444.
34. Giusti, A., Cireşan, D.C., Masci, J., Gambardella, L.M. and Schmidhuber, J., 2013, Fast image scanning with deep max-pooling convolutional neural networks. In IEEE International Conference on Image Processing, pp. 4034-4038.
35. Zeiler, M. D., & Fergus, R. (2014). Visualizing and understanding convolutional networks. In Proceedings of the European Conference on Computer Vision, pp. 818–833.
36. Szegedy, C., Liu, W., Jia, Y., Sermanet, P., Reed, S., Anguelov, D., ...Rabinovich, A. (2015). Going deeper with convolutions. In Proceedings of the IEEE Conference on Computer Vision and Pattern Recognition, pp. 1–9.
37. <https://wiki.cancerimagingarchive.net/display/Public/LIDC-IDRI>
38. Quan Huynh-Thu and Mohammed Ghanbari. Scope of validity of PSNR in image/video quality assessment. Electronics letters, 44(13), pp. 800–801, 2008.
39. Bharodiya, A.K. and Gonsai, A.M., 2019. An improved edge detection algorithm for X-Ray images based on the statistical range. Heliyon, 5(10), p.e02743.
40. Javier López-Randulfe, CésarVeiga, Juan J Rodríguez-Andina, and JoséFariña. A quantitative method for selecting denoising filters, based on a new edge-sensitive metric. IEEE International Conference on Industrial Technology (ICIT), pp. 974–979, 2017.
41. Dhanalakshmi. Pand Satyavathy.G., "Fuzzy Bat Algorithm based Segmentation and Mean Weight Convolution Neural Network (MWCNN) Classification for Lung Images", International Journal of Psychosocial Rehabilitation, Vol. 24, Issue 05, PP. 3781-3794, 2020